AD NUMBER
AD043331
CLASSIFICATION CHANGES
TO: **unclassified**
FROM: **confidential**
LIMITATION CHANGES
TO: **Approved for public release; distribution is unlimited.**
FROM: **Distribution authorized to DoD only; Administrative/Operational Use; 28 FEB 1954. Other requests shall be referred to Bureau of Ships (Navy), Washington, DC 20350.**
AUTHORITY
BUSHIPS ltr dtd 1 Apr 1968; BUSHIPS ltr dtd 1 Apr 1968

SPERRY GYROSCOPE COMPANY
DIVISION OF THE SPERRY CORPORATION
GREAT NECK, NEW YORK

CONFIDENTIAL

TWELFTH INTERIM DEVELOPMENT REPORT
ON
STUDY OF TECHNIQUES FOR MEASURING MICROWAVE HIGH-POWER BREAKDOWN IN WAVEGUIDE TRANSMISSION LINES

THIS REPORT COVERS THE PERIOD DEC. 1, 1953 TO FEB. 28, 1954

SPERRY GYROSCOPE COMPANY
DIVISION OF THE SPERRY CORPORATION
GREAT NECK, NEW YORK

NAVY DEPARTMENT, BUREAU OF SHIPS, ELECTRONICS DIVISION
CONTRACT NObsr-52227, INDEX NO. NE-110607

SPERRY REPORT
NO. 5224-1347

COPY NO. 3
MARCH 1954

CONFIDENTIAL

ABSTRACT

A series of tests was made to determine the peak-power capacity of 1 x 1/2 x 0.050-inch waveguide components. In these tests the gas pressure was varied, and the data was plotted in the form of log power vs. log pressure.

In most cases a straight line resulted, indicating that breakdown power is an exponential function of the pressure. However, in a test made on a vertebrae section of waveguide a curve having two slopes resulted, suggesting the possibility of two distinct types of breakdown. In addition, the data from the tests made on a TM_{01} mode rotary joint resulted in a curve whose slope changed from 2.0 to 1.0 and then back to 2.0 again. This type of phenomenon suggests the possibility of a transition region in which Paschen's Law may not apply.

Peak-power breakdown investigations were conducted on the following: a waveguide section containing a gap in the broad wall of a waveguide, a hemispherical-bump section or spark gap, a vertebrae (flexible waveguide), a 90-degree H-plane bend, a mechanical waveguide switch and dummy load, an E-plane hybrid ring, the effect of mechanical finish, a TM_{01} rectangular-to-circular waveguide rotary joint, an antenna assembly, and a longitudinal serrated choke.

TABLE OF CONTENTS

TABLE OF CONTENTS (Cont.)

LIST OF ILLUSTRATIONS*

- - - - - - -

*Illustrations are grouped in numerical order at the rear of this report.

LIST OF ILLUSTRATIONS (Cont.)

PART I

SECTION A

PURPOSE

1. PURPOSE OF DEVELOPMENT

This contract is primarily concerned with the development of a measurement technique to determine waveguide peak-power capacity as a function of several electrical and mechanical variables. A secondary purpose involves the determination of the peak-power capacity of specified components in 3 x 1-1/2 x 0.080-inch and 1 x 1/2 x 0.050-inch waveguide.

2. STUDY AND WORK PHASES

The course of the program is such that the following points will be particularly stressed:

a. Study and full appraisal of all available technical information on the subject of breakdown in waveguide transmission lines and components.

b. Study and experimental investigation of various means for the positive measurement of peak-power capacity.

c. Development of the techniques required for the application of the method of measurement chosen from b.

d. Investigation into the problem of determining the breakdown region.

e. Application of the results of the previously described work to an investigation of the dependence of peak-power capacity upon the following design parameters:

(1) pulse duration
(2) pulse shape
(3) pulse-repetition frequency
(4) gas pressure
(5) nature of the gas
(6) mechanical finish
(7) plating material
(8) microwave frequency

f. The 1 x 1/2 x 0.050-inch waveguide components to be tested shall include the following:

(1) DA-22/U Termination
(2) CU-206/U Directional Coupler
(3) CU-164/U Interlocked Flexible Waveguide
(4) CU-168/U Convoluted Flexible Waveguide
(5) UG-446/U Waveguide-to-Type N Adapter
(6) UG-456/U Series Tee
(7) UG-457/U Shunt Tee
(8) UG-40A/U-to-UG-39/U, Choke-to-Cover Flange Connection

(9) UG-39/U-to-UG-39/U, Cover-to-Cover Flange Connection

(10) Rotating Joint, Circular-Waveguide Type

(11) Rotating Joint, Rectangular-Waveguide Type

(12) Directional Coupler, Branch-Guide, 10-db

(13) Directional Coupler, Two-Hole, 20-db

(14) Directional Coupler, Bethe-Hole, 25-db

(15) Directional Coupler, Long-Slot, 10-db

(16) Directional Coupler, Schwinger, 30-db

(17) Waveguide Switch, Rotating-Drive Type

(18) Waveguide Switch, Resonant-Ring Type

(19) Waveguide Switch, Rotating-Disc Type

(20) Hybrid-Ring Duplexer

(21) Conventional Waveguide Duplexer

3. PROJECT PERFORMANCE AND SCHEDULE

Figure 28 gives a graphical breakdown of the work performed on this project to date, and the anticipated schedule for the various phases to be completed.

SECTION B

GENERAL FACTUAL DATA

4. REFERENCES

First through tenth interim reports on Study of Techniques for Measuring Microwave High-Power Breakdown in Waveguide Transmission Lines, furnished by Sperry Gyroscope Company to Navy Department, Bureau of Ships, Electronics Division, under Contract No. NObsr-52227.

D. Dettinger and R. Wengenroth (Wheeler Laboratories), "A Standard Waveguide Spark Gap," Transaction of I.R.E. Professional Group on Microwave Theory and Techniques, Vol. M.T.T.-1, No. 1, pp. 39-48, March 1953.

G. L. Ragan, Microwave Transmission Circuits, Radiation Laboratory Series, Vol. 9, McGraw-Hill Book Company, Inc., New York, 1948, pp. 403-405.

J. A. Pim, "The Electrical Breakdown Strength of Air at Ultra-High Frequencies", Proceedings of the Institute of Electrical Engineering, Vol. 96, Part III, p. 117, January 1949.

5. ROOT-MEAN-SQUARE TECHNIQUE FOR CLASSIFING SURFACE ROUGHNESS

The root-mean-square technique for classifying surface roughness is applicable to machined surfaces only. Surfaces that are produced by casting, molding, forging, rolling or some similar technique cannot be specified by an RMS value.

The term RMS is defined as follows: RMS is the square root of the sum of the squares of n measurements of the heights and depths of the surface divided by n. This definition expressed as a formula becomes:

$$RMS = \sqrt{\frac{A^2 + B^2 + C^2 + D^2 + \ldots + n^2}{n}}$$

The heights and depths of the surface are measured in microinches from a mean surface, that is, an imaginary surface that would occur if the valleys and peaks were averaged to zero. See figure 27 which contains a sketch of a machined surface.

The RMS value is truly representative of a machined surface because it gives appropriate emphasis to the peaks and valleys comprising the surface. The actual readings are taken with a profilometer which consists of a stylus, that runs along the machined surface, connected to an effective reading voltmeter calibrated to read in microinches.

The actual waveguide test sections were fabricated by using a milling tool cutter which was preset to a fixed angle. The roughness of the finish was then varied by varying the feed rate of the work into the tool. In this manner the depth and spacing of the grooves was varied.

SECTION C

DETAIL FACTUAL DATA

6. INTRODUCTION

The survey of all available technical information on the subject of breakdown has been completed. The experimental phase of the work is now well under way. Tests are being made at reduced pressure to induce breakdown; radioactive cobalt is employed to provide the initial free electrons. The test circuit utilizes a Transvar™ coupler to suppress harmonics, a thermistor bridge to measure power, and a photocell to detect breakdown. This circuit was chosen in accordance with a statistical approach to breakdown. This approach has been theoretically justified and experimentally verified.

It has been shown that the effect of external irradiation of the breakdown gap (using radioactive cobalt) is to increase the sparking probability without lowering the power-handling ability of the waveguide. Additional tests have shown that the breakdown power for standard rectangular waveguide is proportional to the square of the pressure.

The Eleventh Interim Report presented data relating the effects, on breakdown power, of misaligning a choke-to-cover flange connection. It was found that a misaligned

choke-to-cover flange connection carried more power than an equally misaligned cover-to-cover flange connection. In addition, tests were made to determine the peak-power capacity of Titeflex flexible waveguide, waveguide sections containing hempspherical bumps, and waveguide sections containing grooves and gaps.

7. BREAKDOWN TESTS ON A WAVEGUIDE SECTION WITH A GAP IN THE BROAD WALL

A special test section, shown in figure 1, was constructed to complete the tests on the effects of grooves and gaps in waveguide walls. A section of the broad waveguide wall was removed and a plate heliarc welded in its place. No special gap was intended. The gap that occurred is the normal result of this welding process. The dimensions of the removed section were made to correspond to that of standard 1 x 1/2 x 0.050-inch waveguide. In this manner the data can be compared directly with other test results.

The circuit used to measure the breakdown power of the special heliarc-welded test section is the same as that used in previous tests and is shown in figure 2. The data is given in figure 3. It is seen that the curve of log power vs. log pressure is linear and has a slope of 2.1 which is

exactly the same as that of a standard waveguide section. The peak-power capacity at atmospheric pressure is found by extrapolation to be 1.25 megawatts or 93 percent of the full waveguide power. This data agrees fairly well with the results presented in the Eleventh Interim Report on the specially constructed section used to simulate gaps and grooves in waveguide walls. The difference in the power capacity is partly due to the slightly rough surface around the gap and partly due to experimental error.

8. CLARIFICATION OF THE DATA ON HELIARC-WELDED TEST SECTIONS

In the Eleventh Interim Report, breakdown data was presented on a specially constructed section used to simulate grooves and gaps in waveguide walls. These tests indicated that the unit, with a groove of 0.041 inch in the broad wall and 0.037 inch in the narrow wall and with a gap of 0.016 inch, would carry full waveguide power. Test pieces were manufactured and, since the desired dimensions were difficult to maintain, the pieces were dissected in order to explain the difference in peak-power capacity.

Figure 4 is a photograph of the cross section of the typical heliarc-welded butt joint which carried 73 percent of the full waveguide power. The photograph shows that there is

a misalignment and a small gap at the juncture in both the narrow and broad waveguide walls. Figure 5 is a photograph of the cross section of the welded collar butt joint having a 0.005-inch gap. In this case, the juncture contains no misalignment although there is a small gap between the mating surfaces. This unit carried 88 percent of the full waveguide power.

Figure 6 is a photograph of the cross section of the typical heliarc-welded choke joint which carried 68 percent of the full waveguide power. The photograph shows that the surface finish is rough and that a part of the welding agent dropped down into the waveguide. In addition, there is a small gap at the juncture of the waveguide to the flange. Because of these factors a carrying capacity of 68 percent of the full waveguide power appears to be justified.

Figure 7 is a photograph of the cross section of the heliarc-welded choke joint having a 0.005-inch gap. Here the surface finish is smoother but again some of the welding agent dropped down into the waveguide. The gap between the waveguide and the choke flange is noticeably larger than in figure 6 and there is a slight misalignment at the juncture in the broad wall of the waveguide. Although these conditions have some effect in lowering the peak-power capacity to 58

percent of the full waveguide power, the conditions causing the appearance of the dual-slope curve have the major effect. If the initial curve of the dual-slope curve shown in figure 21 of the Eleventh Interim Report had continued, it would have resulted in a peak-power capacity of 92 percent of the full waveguide power. Since little is known of the reason for the dual-slope curve, all comments will be withheld until such time as more information has been obtained on this phenomenon.

9. BREAKDOWN TESTS ON SECTIONS CONTAINING HEMISPHERICAL BUMPS

In the preceding quarter, an investigation on waveguide sections containing hemispherical bumps was begun. (Refer to the Eleventh Interim Report.) To further supplement this information and to examine more closely the breakdown of a basic microwave structure, tests were conducted on a bump with a radius of 0.150 inch.

The test circuit used to measure breakdown is shown in figure 2. The test piece was a standard 1 x 1/2 x 0.050-inch waveguide with the hemispherical bumps inserted as shown in figure 8. The results of the tests on the 0.150-inch bump radius and a replot of the data taken previously, for the

0.050-inch and 0.100-inch radii, are shown in figure 8. It can be seen that the slopes of the three curves are essentially constant at approximately 1.7 and the power-carrying ability decreases as the bump radius is increased. For the 0.150-inch radius, the peak-power capacity is seen to be 0.135 megawatt or 10 percent of the full waveguide power.

The fact that the slope remains constant as the bump radius is increased indicates that the field pattern remains constant over the range of radii tested, which agrees with the low-frequency analogy presented by Wheeler Laboratories.* This means that the power-handling ability is reduced as the bump radius is increased, for a constant breakdown gradient. In addition, figure 8 shows that the slope of the log power vs. log pressure curve remains constant in the pressure range from 11 to 40 inches of mercury (absolute pressure) which represents a greater range than previously reported.

10. BREAKDOWN TESTS ON A VERTEBRAE SECTION OF WAVEGUIDE

Tests were made on a Technicraft Laboratories Flexible Waveguide Assembly No. U64-65B vertebrae in standard

- - - - - - -

*D. Dettinger and R. Wengenroth (Wheeler Laboratories), "A Standard Waveguide Spark Gap," Transaction of I.R.E. Professional Group on Microwave Theory and Techniques, Vol. M.T.T.-1, pp. 39-48, March 1953.

1 x 1/2 x 0.050-inch waveguide. The construction features of this type of flexible waveguide are shown in figure 9. This unit consists of a series of quarter-wavelength sections separated by choke-to-cover flange joints housed in a rubber jacket. Electrical continuity is maintained by means of the choke-to-cover connection even though the unit is flexed. The gaps allow relative motion of the sections.

The test circuit is shown in figure 2. The results of the tests, shown in figure 10, consist of a curve with two slopes, 2.0 and 1.5. The two slopes were averaged to give a slope of 1.72 and this curve is also shown in figure 10. The peak-power capacity at atmospheric pressure was found, by extrapolation of the average slope curve, to be 54 percent of the full waveguide power. The appearance of the dual-slope curve was not too unexpected since the construction of the vertebrae produces choke-to-cover connection misalignments of a type that have previously resulted in a dual-slope curve. (See the Eleventh Interim Report.)

11. BREAKDOWN TESTS ON A 90-DEGREE H-PLANE BEND

Tests were performed on a 90-degree H-plane bend in standard 1 x 1/2 x 0.050-inch waveguide having a radius of 0.300 inch. (See figure 11).

The test circuit used is shown in figure 2. The results of the test are plotted in figure 11. The curve obtained has a slope of 2.0 which is approximately the same as that for standard waveguide. Extrapolation indicates that the bend will carry 82 percent of the full waveguide power at atmospheric pressure. Further comments will be deferred to the next interim report which will contain more complete information on the peak-power capacity of waveguide bends, corners, and twists.

12. BREAKDOWN TESTS ON A WAVEGUIDE SWITCH AND DUMMY LOAD

Tests were performed on the mechanically rotated waveguide switch shown in figure 12. As shown in the drawing, the switch consists of a rotor, containing a 90-degree E-plane bend, separated from the stator by a nominal 0.003-inch gap. A set of choke slots have been machined into the stator to increase the peak-power capacity by decreasing the effect of the gap. The switch uses standard 1-1/4 x 5/8 x 0.064-inch waveguide.

The test circuit used to measure breakdown is shown in figure 2 with the exception that the dummy load is part of the test piece. The data obtained is shown in figure 13. It can be seen from this figure that the slope of the log

power vs. log pressure curve is 1.9. The peak-power capacity of the waveguide switch and dummy load at atmospheric pressure is found, by extrapolation, to be 39 percent of 1-1/4 x 5/8 x 0.064-inch waveguide power. (For a first order approximation, the peak-power capacity of 1-1/4 x 5/8 x 0.064-inch waveguide is 2.7 megawatts at atmospheric pressure, twice that of 1 x 1/2 x 0.050-inch waveguide). Since previous experience has shown (refer to Eighth Interim Report) that the breakdown characteristics of dummy loads is erratic, it is difficult to evaluate this data properly with the information now available. However, breakdown data will be taken in the next quarter on E-plane bends and this will permit a re-evaluation of present data in the next report.

13. BREAKDOWN TEST ON AN E-PLANE HYBRID RING

A 1 x 1/2 x 0.050-inch E-plane hybrid ring, shown in figure 14, was tested. As indicated on the drawing the b dimension of the inner ring is reduced to 0.281 inch. This is done principally for matching purposes. Operation of the unit is such that the power fed into terminal 1 is split equally between terminals 2 and 4 with terminal 3 isolated by approximately 30 or 40 db from the input power. This operation is similar to that of a magic tee, with terminals 1 and

3 acting as the E and H arms and terminals 2 and 4 as the side arms.

The test circuit used to measure the breakdown power is shown in figure 2. From the data plotted in figure 15, the slope of the log power vs. log pressure curve is seen to be 1.6. By means of extrapolation, the peak-power capacity at atmospheric pressure is found to be 0.25 megawatt or 19 percent of the full waveguide power. This performance is similiar to that of an E-plane tee junction, as expected. (In figure 5 of the Ninth Interim Report, it was seen that the E-plane tee carried 0.09 megawatt at atmospheric pressure and the slope of the log power vs. log pressure curve was 1.30.)

14. BREAKDOWN TESTS ON THE EFFECT OF MECHANICAL FINISH

Three pieces of waveguide were fabricated with different values of roughness on all four walls in order to investigate the effect of surface roughness on peak-power capacity. (The definition and measurement of an RMS finish is contained in paragraph 5.) After the completion of the tests the RMS values of the pieces were measured and found to be as follows:

a. Piece number one varied from 300 to 400 RMS
b. Piece number two varied from 550 to 650 RMS
c. Piece number three varied from 650 to 850 RMS.

Since these values are higher than those normally encountered, they represent an extreme condition of surface roughness and as such form an upper limit, above which no practical application exists. For example, drawn brass waveguide is generally better than 64 RMS. These tests were valuable since the data indicated breakdown values which are considerably better than those of most waveguide components.

The circuit used to determine the breakdown power is shown in figure 2. The data on the three test pieces is plotted in figures 16, 17, and 18. As shown in the figures, the slope of the log power vs. log pressure curves remains essentially constant at 2.0, which is the same as the slope for a standard waveguide section. By extrapolation of the curves, the peak-power capacity at atmospheric pressure is found to be as follows:

a. Piece number one (300-400 RMS) - 91 percent of the full waveguide power, or 1.23 megawatt.

b. Piece number two (550-650 RMS) - 84 percent of the full waveguide power, or 1.14 megawatt.

c. Piece number three (650-850 RMS) - 76 percent of the full waveguide power, or 1.03 megawatt.

Thus it is seen that the 300-400 RMS finish, which is worse than that generally encountered in practice, will carry 91 percent of the full waveguide power. This is considerably more power than most waveguide components will carry and enables a relaxation of surface finish specifications on many components.

15. BREAKDOWN TESTS ON A RECTANGULAR-TO*CIRCULAR WAVEGUIDE ROTARY JOINT

The unit selected for test was a TM_{01} mode rectangular-to-circular waveguide rotary joint. Figure 19 consists of a sketch showing the pertinent dimensions of the joint. As shown in the sketch, the joint consists of two individual half sections. Each half section contains a rectangular-to-circular waveguide transition (TE_{10} to TM_{01}). Each half section also contains a filter ring and absorbing slots to eliminate any TE_{11} wave which may be generated by the transition. The TE_{11} wave must be eliminated because it will propagate in the circular waveguide and impair the performance of the joint. Due to the addition of the filter ring, an inductive iris had to be added to provide a match at the transition and thereby keep the VSWR relatively low. Figure 20 consists of a curve of VSWR vs. frequency for the rotary joint tested. At the frequency used in the test (9375 mc) the VSWR is 1.09.

The circuit used to measure the breakdown power is shown in figure 2. Because of the geometry of the rotary joint, the use of the photocell to indicate breakdown was greatly limited and much time and care had to be used in obtaining the data. Each point had to be checked several times to make sure of its reliability. Figure 21 consists of a plot of the data obtained. As shown in the figure, an entirely different type of phenomena was observed. On plotting the log power vs. log pressure relationship, two distinct constant-slope curves resulted. Each curve has the same slope, which is essentially that of standard waveguide, but the curves are displaced from one another. Since these points cannot be averaged to give a single curve, as done previously, the performance at atmospheric pressure was obtained by extending the upper, or high-power, portion of the data. Thus, the peak-power capacity at atmospheric pressure is found to be 14 percent of the full waveguide power or 0.193 megawatt.

16. BREAKDOWN TESTS ON AN ANTENNA ASSEMBLY

The antenna assembly shown in figure 22 was selected for breakdown-power tests. Basically the unit consists of a waveguide section twisted 90 degrees, a matching screw and iris, and a transition from rectangular-to-circular waveguide.

(See figure 23.) A solid Teflon cylinder is mounted in the circular guide to enable the waveguide to be pressurized and also to protect the waveguide from the elements. The antenna itself consists of a parabolic reflector, or dish, which was used during the test to ensure a good match at the input to the antenna assembly (since this is how the antenna assembly was originally matched). The VSWR at the test frequency (9375 mc) is 1.10.

Figure 2 shows the test circuit used to measure the breakdown power. A log power vs. log pressure curve was not taken on this component since it could not be evacuated due to the fact that it was an experimental model and had several air holes in the solder joints. Here again the point of onset stress was difficult to obtain, for the geometry of the unit made it difficult to detect breakdown with the photocell. The test data indicated that the antenna assembly would carry 0.224 megawatt at atmospheric pressure.

17. BREAKDOWN TESTS ON A LONGITUDINAL SERRATED CHOKE

Since it is necessary to utilize a longitudinal choke in the construction of certain microwave components (such as Transvar rotational joints and Foster-Scanner phase shifters), measurements were made on a serrated longitudinal

choke. Figure 24 consists of a sketch of the unit tested together with the dimensional variations used. The operation of the choke is explained as follows: The region between the bottom plate and choke will act as a parallel-plane transmission line. Therefore, the length of the choke is made equal to a quarter wavelength in air and electrical continuity is achieved at the inside surface of the waveguide. The chokes are serrated to reduce the propagation of extraneous modes which would result in a loss of power. The width of the choke sections is made equal to one quarter of the waveguide wavelength to match the choke sections to the main waveguide. The VSWR for the unit is under 1.10.

The test circuit used to measure the breakdown power is shown in figure 2. A log power vs. log pressure relationship was not plotted because the test unit could not be pressurized. Therefore, the tests were performed at atmospheric pressure. The data showed that the serrated choke test unit had a power-handling ability greater than 0.230 megawatt. This power-handling ability remained unchanged for all the dimensional variations listed in figure 24.

18. ASSEMBLY OF THE 3000-MC TEST CIRCUIT

The program to determine the power-handling ability of 3 x 1-1/2 x 0.080-inch waveguide components has been

delayed due to further difficulties with the power source. It is anticipated that the tube will not be available until the end of the next quarter. In the meantime, another power source with a lower power output has been obtained. This source will be used to develop the necessary test circuitry and to obtain as much data as the limited power level permits.

19. GENERAL DISCUSSION OF DATA

The information on the effects of gaps and grooves in waveguide walls, on peak-power capacity, indicates that heliarc-welding techniques are perfectly feasible for fabrication of waveguide components. (The discrepancy that existed in the data between the specially constructed test section and the actual heliarc-welded units is qualitatively explained in paragraph 8.) It has been shown (with the exception of the choke weld having a 0.005-inch gap) that power capacities of 70 percent of the full waveguide power and higher can be realized in heliarc-welded components without resorting to special manufacturing precautions. Power-handling abilities of the order of 90 percent of the full waveguide power can be realized if special steps are taken to ensure proper alignment of mating surfaces and a reasonably smooth surface finish is maintained. Since practically all microwave components have peak-power

capacities less than 70 or 90 percent of the full waveguide power, the use of this heliarc-welding technique is permissible and will not lower the peak-power capacity of any component. With the trend toward making radar systems lighter by using aluminum in the construction of waveguide components, the use of heliarc welding will greatly reduce the cost of such systems.

In the case of the heliarc-welded choke joint having a 0.005-inch gap, the data obtained can be compared with that contained in figure 6 of the Eleventh Interim Report on the misalignment of a choke-to-cover flange. In both tests a plot of the data results in a dual-slope curve. For the choke weld having a 0.005-inch gap, the slopes of the log power vs. log pressure curves are 2.03 and 1.3, with a peak-power capacity, at atmospheric pressure, of 60 percent of the full waveguide power. The data on the misaligned choke-to-cover flange yielded log power vs. log pressure curves with slopes of 2.07 and 1.56, with a peak-power capacity of 70 percent of the full waveguide power. It is surmised that the gap in the back end of the flange of the choke weld, shown in figure 7, resulted in a current breakdown and thereby lowered the slope of the log power vs. log pressure curve to 1.3. However, because of a lack of

information on this phenomenon, no definite conclusions can be drawn until more tests have been conducted.

Several interesting effects may be observed in the data on the waveguide section containing a hemispherical bump. First, the information reported by Wheeler Laboratories, that a section containing a 0.100-inch radius bump will carry 7.5 percent of the full waveguide power, has been reasonably verified by the data obtained in the eleventh quarter. The data indicates a peak-power capacity of 13.3 percent of the full waveguide power. Second, the statement by Wheeler Laboratories, that this type of bump section would make an excellent spark gap to use as a standard for comparing data taken by various individuals throughout the country, seems plausible. As they reported, the spark gap breaks down at a comparatively low-power level, is easily matched, and small variations in the dimensions of the bump do not have a pronounced effect upon the peak-power capacity of the unit. (See figure 8.) Third, the fact that the slope of the log power vs. log pressure curve remains constant for various bump radii indicates that the voltage gradient necessary for breakdown remains constant. Thus, as the radius of the bump is increased, the power at which breakdown occurs is decreased so that the voltage gradient remains constant. In order to

predict the decrease in power as the radius of the bump is increased, it is necessary to refer to the appendix to the article by Wheeler Laboratories*.

The solution to the problem of a hemispherical bump in a waveguide is approximated by the standard electrostatic solution for a spherical surface in the vicinity of a charge. The solution for the hemispherical bump problem is given by:

$$E = \frac{q}{4\pi\epsilon} \frac{6}{s^2} = K \frac{q}{s^2} \qquad (1)$$

where,

E = voltage gradient set up by the charge q

q = magnitude of the charge

s = distance from the center of the sphere, or the waveguide surface, to the plane equipotential surface, or the other wall of the waveguide.

For equation (1) to hold,

$$s >> r$$

where,

r = radius of the hemisphere.

- - - - - - -

*D. Dettinger and R. Wengenroth, op. cit.

As a first approximation, the magnitude of the charge q is the only factor in equation (1) that will vary as the bump radius is varied. Since the field distribution is sinusoidal and since the charge q will vary as the surface area of the bump, we may say that q varies as $r^2 \cos \frac{2r}{a}$. (See figure 25.) Therefore, substituting in equation (1) yields:

$$E = K \frac{r^2}{s^2} \left[\cos \frac{2r}{a}\right]$$

Since the power P varies as E^2, to a first approximation the power will vary as $\left[\cos \frac{2r}{a}\right]^2$, for different values of radius r. If actual numbers are inserted for the radii and compared with the test data, the following results are obtained.

Radius (inches)	Percent change in power using 0.050-inch radius as base and approximate equation	Percent change in power using 0.050-inch radius as base and test data
0.050	0	0
0.100	9.3	11.0
0.150	23	32.8

It should be expected that the difference between the percent change using the approximate equation and the percent change obtained by test would increase as the radius is increased, since the approximation was based on the fact that $r << s$.

The use of extrapolation in determining the peak-power capacity at atmospheric pressure from data taken below

atmospheric pressure has been previously justified. The data on the hemispherical-bump section was taken in the range from 8 to 40 inches of mercury (absolute pressure) and all of the curves had a constant slope over this range. Since most of the tests on waveguide components have been made in the range of pressures from 5 to 15 inches of mercury (absolute pressure), the data on the hemispherical-bump section bridges the gap between 15 inches of mercury and atmospheric pressure (30 inches of mercury) and has further justified the use of extrapolation.

The final information to be obtained from the data on a hemispherical-bump section is an overall picture of what happens in the section as the bump radius is increased. The effect of the bump is to distort the electric field in such a manner as to produce a non-uniform field and, therefore, a region of increased gradient. This causes a change in the slope of the log power vs. log pressure curve from 2.07 for standard waveguide to 1.77 for the hemispherical-bump section, thereby decreasing the power-carrying ability. The slope remains constant until the bump radius is sufficiently enlarged to distort the field to the point where the gradient necessary for breakdown is again lowered. This will, in turn, again lower the slope of the log power vs. log pressure curve and, therefore, again decrease the power-carrying ability.

The data obtained on the vertebrae section was expected since its construction closely resembles that of a horizontally and vertically misaligned choke-to-cover flange connection. The amount and type of misalignment will vary from one quarter-wave section to the next as will the gap between them, since the sections are not held very rigidly together. Measurement of the gap indicated an average value of 0.022 inch. Comparison of the data on the vertebrae section with the data on the 0.040-inch vertical and horizontal misalignment of the choke-to-cover flange connection indicates the following:

For the vertebrae section -	Slopes of log power vs. log pressure curve are 1.97 and 1.45
	Power capacity at atmospheric pressure is 54 percent of waveguide power
For the 0.040-inch vertical and horizontal misalignment of the choke-to-cover flange connection. -	Slopes of log power vs. log pressure curve are 2.30 and 1.50
	Power capacity at atmospheric pressure is 76 percent of waveguide power.

It can be seen that the slopes compare very favorably while the power capacity differs by 22 percent. The difference in

power capacity is reasonable since the vertebrae sections have, by virtue of their construction, gaps between mating sections. Gaps between choke-to-cover flange connections in the order of 0.022 inch will greatly reduce the power capacity.

A discussion of the performance of the 90-degree H-plane bends will be witheld until the next interim report when the data on bends, twists, and corners will be analyzed.

The discussion of the 1-1/4 x 5/8 x 0.064-inch waveguide switch and dummy load will also be postponed to the next interim report when the data on E-plane bends is presented.

Since the hybrid ring used for tests is essentially a set of E-plane tees, a comparison of this data with that obtained in the Ninth Interim Report on an E-plane tee is pertinent. The major difference between the two units is that the narrow dimension of the inner race of the hybrid ring is reduced by 29.7 percent. This reduction of the b dimension, done principally to improve the match looking into the hybrid ring, acts to reduce the power-handling ability. The VSWR with all output arms terminated is in the order of 1.20 for the hybrid ring and 1.80 for the E-plane tee. A comparison of the data indicates the following:

E-plane Tee - Slope of log power vs. log pressure curve is 1.3.

Power capacity at atmospheric pressure is 7 percent of waveguide power

VSWR = 1.80

E-plane hybrid ring - Slope of log power vs. log pressure curve is 1.6.

Power capacity at atmospheric pressure is 19 percent of waveguide power

VSWR = 1.20

It can be seen that the slope of the log power vs. log pressure curve is approximately equal for both cases. This is to be expected since the units are almost identical and, therefore, should have the same voltage gradient necessary for breakdown. Reduction of the narrow waveguide dimensions in the hybrid ring by 30 percent should correspondingly reduce the power capacity by 30 percent, since peak-power capacity varies directly with the area. However, an E-plane tee junction reduces the peak-power capacity by considerably more than 30 percent (as evidenced by the data). Therefore, this reduction in the b dimension has no effect upon the peak-power capacity of the hybrid ring. Rather, the difference in the VSWR between the two units accounts for the 12 percent difference in peak-power capacity.

The information obtained about the effect of surface finish upon peak-power capacity is very interesting. A surface finish of RMS value 300-400 was found to carry 91 percent of the full waveguide power with essentially the same slope, for the log power vs. log pressure curve, as standard waveguide. Since RMS values in this region are generally much worse than those encountered in practice, the effect of surface finish upon peak-power capacity is small. To further illustrate this fact a finish with an RMS value as high as 850 was found to carry 76 percent of the full waveguide power; a larger amount of power than most microwave components can handle. However, a word of caution must be inserted. The above data indicates that precautions as to surface finish need not be taken for straight waveguide, since it will still carry 90 percent of the full waveguide power with a 300-400 RMS finish. However, the individual structures in the components themselves will breakdown at a lower power if the finish is allowed to become rough and, since many components in a radar system are marginal, in some cases even a small reduction in power capacity may not be tolerable.

The appearance, in the data on the TM_{01} mode rotary joint, of two distinct curves having the same slope but displaced from one another deserves some comment. In an article

by J. A. Pim* on the breakdown of air at ultra-high frequencies, he discusses the variations in Paschen's Law as the gap width and pressure are varied for a constant frequency of 150 mc. Expressed as a formula, Paschen's law states:

$$E \left[\frac{\text{volts}}{\text{cm}}\right] = f \text{ (pressure x gap width)}$$

$$= f (p\delta)$$

For the data presented in Pim's article, the gap width is the parameter varied to obtain the desired information. Curve A of figure 26 corresponds to the Paschen's law for d-c conditions. Curve B represents the condition that exists when the gap is increased to the point where the positive ions will not be removed during a cycle of energy, but will remain in the gap and change the Paschen law. Curve C occurs when the gap is further increased so that electrons as well as positive ions will oscillate in the gap because they cannot all be removed during a cycle of energy. Curves B and C are very similar to the curve obtained on the rotary joint, as shown in figure 21. Although Pim took the data for variations in gap width, it can also be reasoned by virtue of Paschen's law that the same condition would occur if the pressure were

- - - - - - -

*J. A. Pim, "The Electrical Breakdown Strength of Air at Ultra-High Frequencies", Proceedings of the Institute of Electrical Engineering, Vol. 96, Part III, p. 117, January 1949.

varied while the gap width remained constant. In the TM_{01} rotary joint there are several structures which may act as a gap, for example, the iris, the absorbing slots, or the filter ring. However, more information must be obtained before this phenomenon can be completely analyzed.

In volume nine of the Radiation Laboratory Series*, G. L. Ragan discusses a breakdown test conducted on a rectangular-to-circular waveguide transition containing a matching iris and filter ring. In construction, this unit is similiar to a half section of the TM_{01} rotary joint tested in this quarter. (See figure 19.) Ragan reports that the transition carried a peak power of 0.90 megawatt at atmospheric pressure for a one-microsecond pulse width and a 1000-cps repetition rate. The data obtained in this program indicated a peak-power capacity of 0.193 megawatt at atmospheric pressure for a 1.2-microsecond pulse width and an 800-cps repetition rate. Since it is reasonable to assume that the breakdown power for each half section of the rotary joint will be the same, and that the combination of the two half sections will not significantly reduce the power capacity, there is a fairly large discrepancy between the two sets of

- - - - - - -

*G. L. Ragan, Microwave Transmission Circuits, Radiation Laboratory Series, Vol. 9, New York, McGraw-Hill Book Company, Inc., 1948, pp. 403-405.

data. However the accuracy of the data presented by Ragan is to be questioned. Ragan determined the breakdown power at reduced pressure and extrapolated this point to atmospheric pressure, assuming that the power varied with the pressure raised to the 4/3 power. If the actual pressure at which breakdown occurred, in the transition discussed by Ragan, is determined using the 4/3 power law it is found that the transition is carrying 50 percent more power than standard waveguide will carry. This is not reasonable and casts serious doubts on the data reported by Ragan.

The construction of the antenna assembly (figure 22) indicates that the weakest point, insofar as peak-power capacity is concerned, is the matching screw. Although geometrically the screw is not too similiar to a sphere, it is informative to compare this data with that taken on the hemisperical-bump section. The screw is a 1/4-40 having a 0.250-inch diameter and extending 0.060 inch into the guide. It is located 0.160 inch from the centerline of the waveguide. Because of its sharp edges and increased volume, the screw has a greater effect upon the field than a hemisphere and, therefore, tends to decrease the peak-power capacity. However, the fact that it is displaced 0.160 inch from the centerline of the waveguide will tend to increase its power-handling ability. Taken together, the two effects should tend to

compensate for each other and the screw data should be comparable to that of the hemispherical-bump section. Comparing the data on the screw, inserted 0.060 inch into the waveguide, with that for a 0.050-inch bump radius the following is obtained:

1/4-40 screw having an 0.060-inch insertion	Power capacity of 0.224 megawatt at atmospheric pressure.
0.050-inch radius hemisphere	Power capacity of 0.20 megawatt at atmospheric pressure.

It is seen that the data compares favorably and, therefore, the assumption that the screw will act as a hemispherical-bump section presents a fairly good approximation.

The data on the longitudinal serrated chokes indicates the feasibility of using this type of choke for high-power radar components. It was unfortunate that the test unit could not be evacuated since at atmospheric pressure it withstood all the power available from the magnetron. It is pertinent to note that this type of choke is used in Transvar rotating joints and, since these chokes are probably one of the weakest links, it is advantageous to know their breakdown power.

SECTION D

CONCLUSIONS

20. GENERAL CONCLUSIONS

Breakdown tests were made on a section containing a 0.150-inch hemispherical-bump radius, a vertebrae section, a 90-degree H-plane bend, a waveguide switch and dummy load, a waveguide hybrid ring, a TM_{01} rotary joint (rectangular-to-circular waveguide), an antenna assembly, and a longitudinal serrated choke. Breakdown tests were also made on the effect of mechanical surface finish and on the effect of a gap in the broad wall of a waveguide.

The tests on the gap in the broad wall of a waveguide indicated a power-carrying ability at atmospheric pressure of 93 percent of the full waveguide power. This completes the analysis of the effect of heliarc-welding techniques on peak-power capacity. It was found that the ordinary use of heliarc welding does not decrease the peak-power capacity to a level lower than 70 percent of the full waveguide power. If special care is taken, power capacities of the order of 90 percent of the full waveguide power can be achieved. Since the power capacity of most microwave components falls below these figures, heliarc welding can

be utilized, thus saving considerable time and money in the fabrication of high-power radar systems.

The breakdown tests on the section having a hemispherical bump with a radius of .0.150 inch indicated a slope of 1.7 for the log power vs. log pressure curve and a power capacity at atmospheric pressure of 0.135 megawatt, or 10 percent of the full waveguide power. This completes the series of tests made on hemispherical-bump sections. The data obtained agreed reasonably well with that reported by Wheeler Laboratories and gave some insight into the breakdown characteristics of basic microwave structures.

Tests on the peak-power capacity of a vertebrae section resulted in a dual-slope curve similar to that obtained for a choke-to-cover flange misalignment. It was found that the average slope of the log power vs. log pressure curve was 1.7 and the power capacity at atmospheric pressure was 54 percent of the full waveguide power, or 0.73 megawatt. Due to the construction of the vertebrae it was expected that the data obtained would resemble that of a misaligned choke-to-cover flange. The slopes of the log power vs. log pressure curves showed this similarity. The lower power capacity of the vertebrae, as compared to the misaligned choke-to-cover

flange, is due to the gap between the quarter-wave sections used in the construction of a vertebrae.

The breakdown tests on the 90-degree H-plane bend indicated a power capacity at atmospheric pressure of 82 percent of the full waveguide power, or 1.10 megawatt, with a slope of 2.0 for the log power vs. log pressure curve.

Tests on the mechanical waveguide switch and dummy load indicated a peak-power capacity at atmospheric pressure of 1.05 megawatt, or 39 percent of the full waveguide power, with a slope of 1.9 for the log power vs. log pressure curve.

The breakdown tests on the E-plane hybrid ring indicated a slope of 1.6 for the log power vs. log pressure curve with a peak-power capacity at atmospheric pressure of 19 percent of the full waveguide power, or 0.256 megawatt. Although the narrow dimension on the inner race of the hybrid ring was reduced, this was not the cause of breakdown. Rather, the distortion of the field due to the E-plane junction was the major factor. Because of this, the data on the hybrid ring was compared to that for the E-plane tee (Ninth Interim Report), and the results of the comparison were favorable. The slope of the log power vs. log pressure curve for the two units was approximately the same and the peak-power capacity

was greater for the hybrid ring (7 percent as compared to 19 percent). This difference in power capacity is mainly due to the lower VSWR that exists in the hybrid ring (1.2 as compared to 1.8).

Tests on the effect of mechanical surface finishes (on all four waveguide walls) on peak-power capacity indicated that an RMS 300-400 finish carries 91 percent of the full waveguide power with essentially the same slope for the log power vs. log pressure curve as that of standard waveguide. A finish as rough as RMS 650-850 carried 76 percent of the full waveguide power with the same slope for the log power vs. log pressure curve as standard waveguide. Since most components do not have power ratings this high, the effect of mechanical finish on regular waveguide sections is negligible. However, it must be noted that since many components in a high-power radar system are marginal a small decrease in peak-power capacity due to surface roughness may not be tolerable in the component.

The breakdown tests on the TM_{01} rotary joint produced a result which had not been encountered previously in this program. The log power vs. log pressure curve consists of two regions of constant slope separated by a range of pressure wherein the power was independent of the pressure.

As indicated in an article by J.A. Pim, this phenomena may be due to the following conditions. At pressures below the break in the curve, some positive ions remain in the gap because their mass inhibits removal during a cycle of energy. At pressures above the break in the curve some electrons as well as positive ions will remain in the gap. This does not violate Paschen's law, that E (volts/cm) = f (pressure x gap width), but merely indicates the presence of a transition region. The TM_{01} rotary joint contains several gaps which may behave as described above but more data must be obtained before this phenomena can be completely analyzed. The slope of both curves of log power vs. log pressure is 2.0 and the peak-power capacity at atmospheric pressure is 0.193 megawatt, or 14.2 percent of the full waveguide power.

Tests on the antenna assembly indicated a peak-power capacity of 0.224 megawatt at atmospheric pressure. A curve of log power vs. log pressure was not plotted because the unit could not be pressurized. It should be noted that if the weakest basic structure in an assembly is known and the breakdown characteristics of this structure have been obtained then the performance of the whole assembly can be predicted quite accurately. In the antenna assembly, the weakest structure is a matching screw located slightly off

the centerline of the waveguide. By making several assumptions and allowing for the difference in geometry the performance of this assembly can be predicted by examining the results of the hemispherical-bump sections. The data for the corresponding size bump radius indicated a power capacity of 0.20 megawatt at atmospheric pressure, which is close to the measured value for the antenna.

The longitudinal serrated chokes had a peak-power capacity at atmospheric pressure of greater than 0.230 megawatt. Since the test unit could not be pressurized, a curve of log power vs. log pressure was not obtained and the actual power capacity at atmospheric pressure could not be determined.

PART II

PROGRAM FOR THE NEXT INTERVAL

21. PROGRAM FOR THE THIRTEENTH QUARTER

Tests on the required 1 x 1/2 x 0.050-inch waveguide components will continue. Tests will begin, using the alternate power source, on the 3 x 1-1/2 x 0.080-inch waveguide size.

Tests will be made to determine the effects of VSWR on peak-power capacity in 1 x 1/2 x 0.050-inch waveguide.

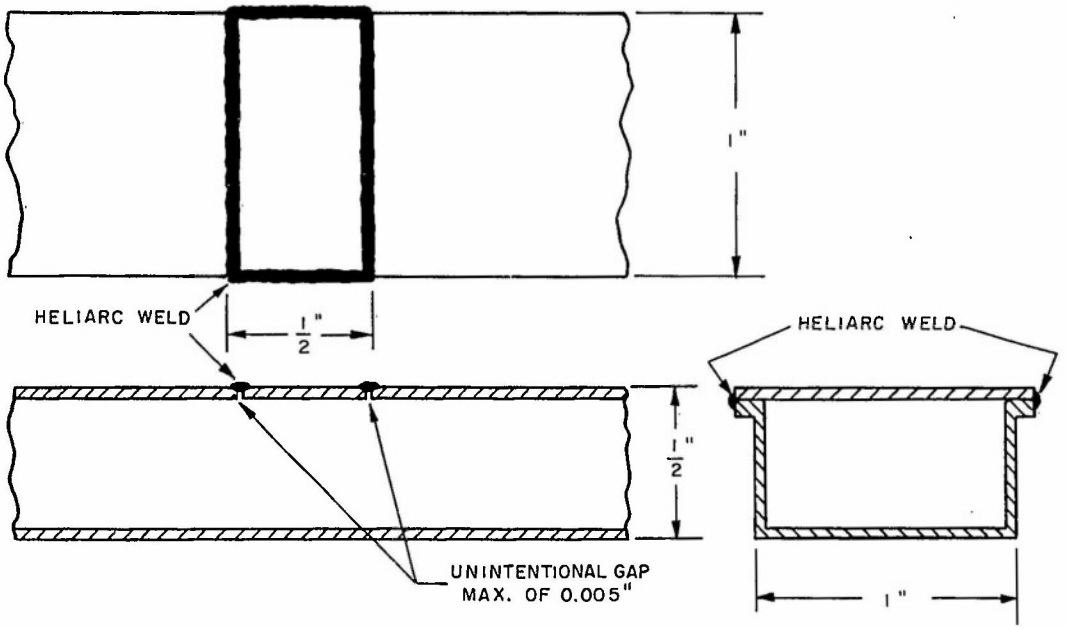

FIGURE 1
HELIARC WELDED TEST SECTION

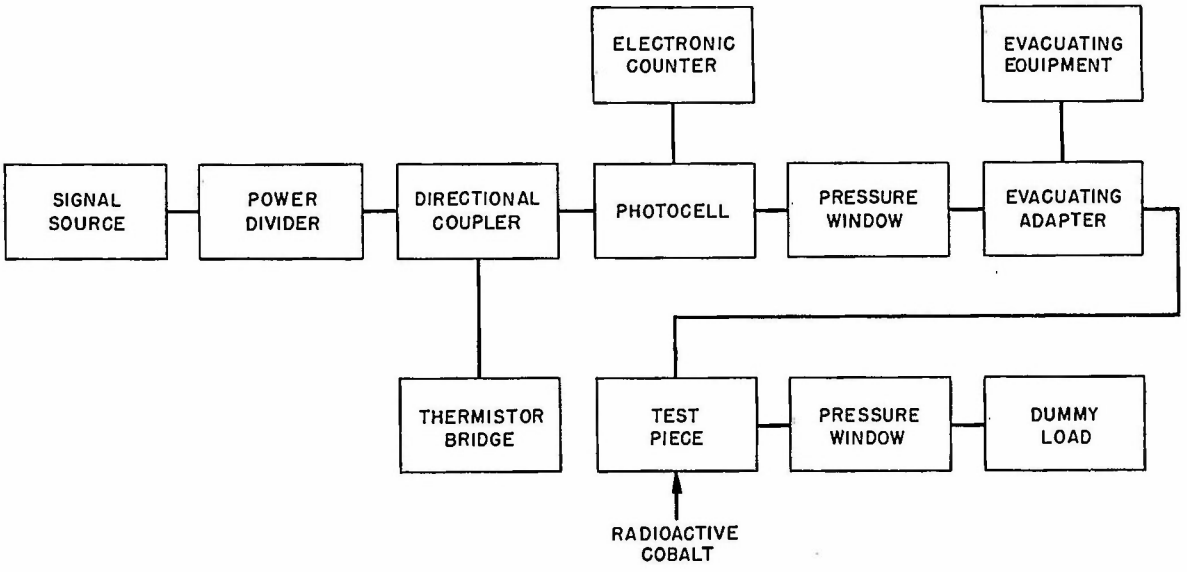

FIGURE 2
BASIC CIRCUIT TO MEASURE
BREAKDOWN OF TEST PIECE

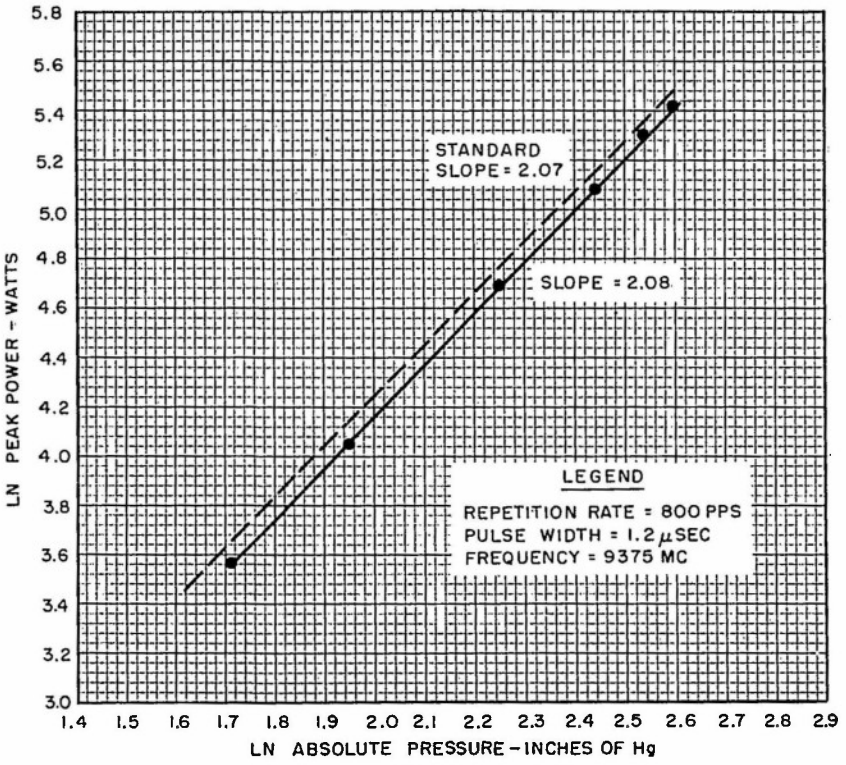

FIGURE 3

POWER VS PRESSURE FOR
HELIARC-WELDED TEST SECTION
(1"X 1/2"X0.050 WAVEGUIDE)

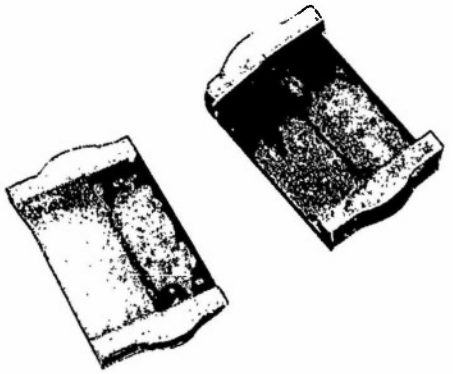

FIGURE 4

PHOTOGRAPH OF CROSS SECTION OF
TYPICAL WELDED BUTT JOINT
(1"X 1/2"X 0.050 WAVEGUIDE)

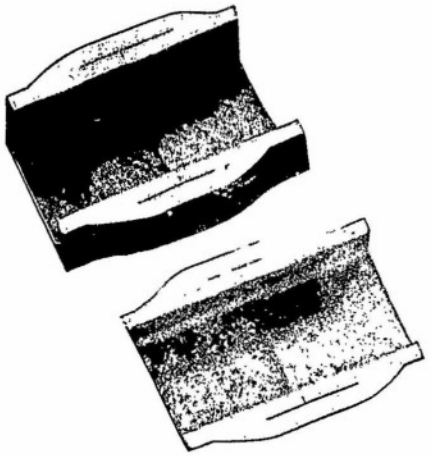

FIGURE 5

PHOTOGRAPH OF CROSS SECTION OF
WELDED COLLAR BUTT JOINT HAVING A 0.005" GAP
(1"X 1/2"X 0.050" WAVEGUIDE)

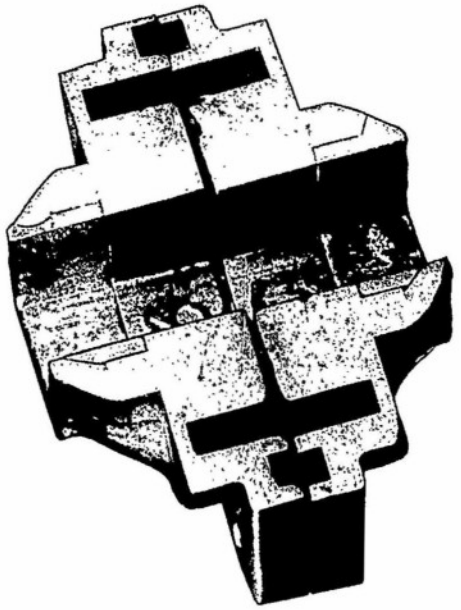

FIGURE 6

PHOTOGRAPH OF CROSS SECTION OF
TYPICAL WELDED CHOKE JOINT
(1"X 1/2"X 0.050" WAVEGUIDE)

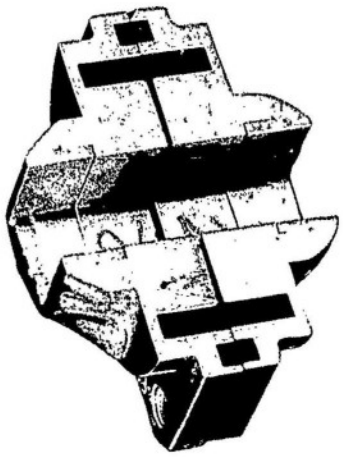

FIGURE 7

PHOTOGRAPH OF CROSS SECTION OF
WELDED CHOKE JOINT HAVING A 0.005"GAP
(1"X 1/2" X 0.050" WAVEGUIDE)

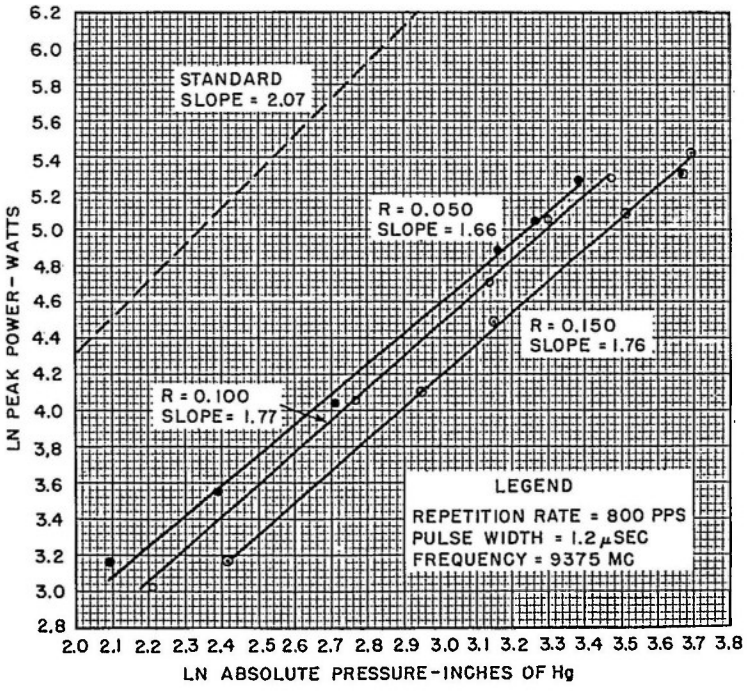

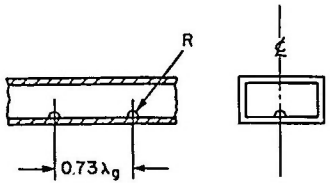

FIGURE 8

POWER VS PRESSURE FOR SECTION
CONTAINING HEMISPHERICAL BUMPS
(1"X 1/2"X 0.050" WAVEGUIDE)

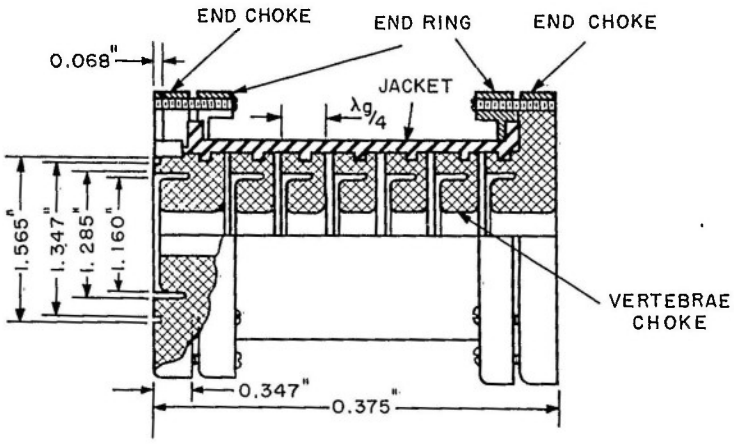

O.D. OF WAVEGUIDE = 1" X 1/2"

FIGURE 9

CONSTRUCTION FEATURES OF VERTEBRAE-TYPE FLEXIBLE WAVEGUIDE

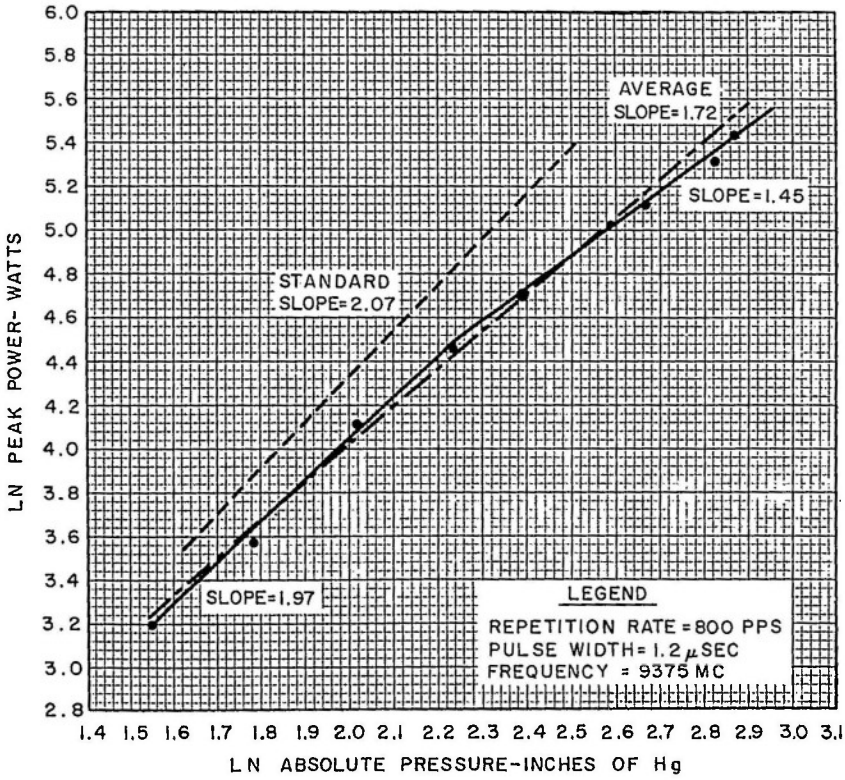

FIGURE 10

POWER VS PRESSURE FOR VERTEBRAE TYPE FLEXIBLE WAVEGUIDE (1"X 1/2"X0.050" WAVEGUIDE)

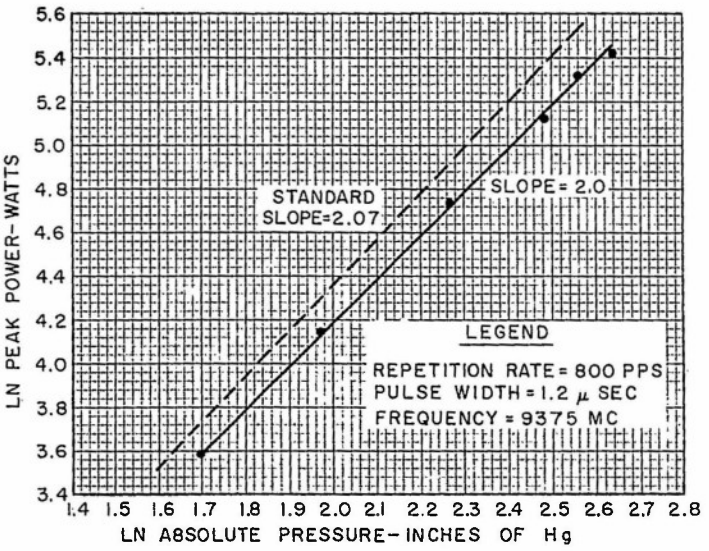

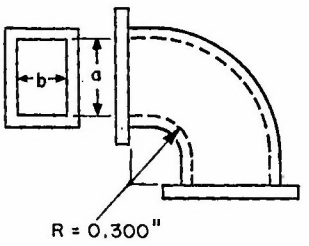

FIGURE 11

POWER VS PRESSURE FOR 90-DEGREE H-PLANE BEND (1"X1/2"X0.050" WAVEGUIDE

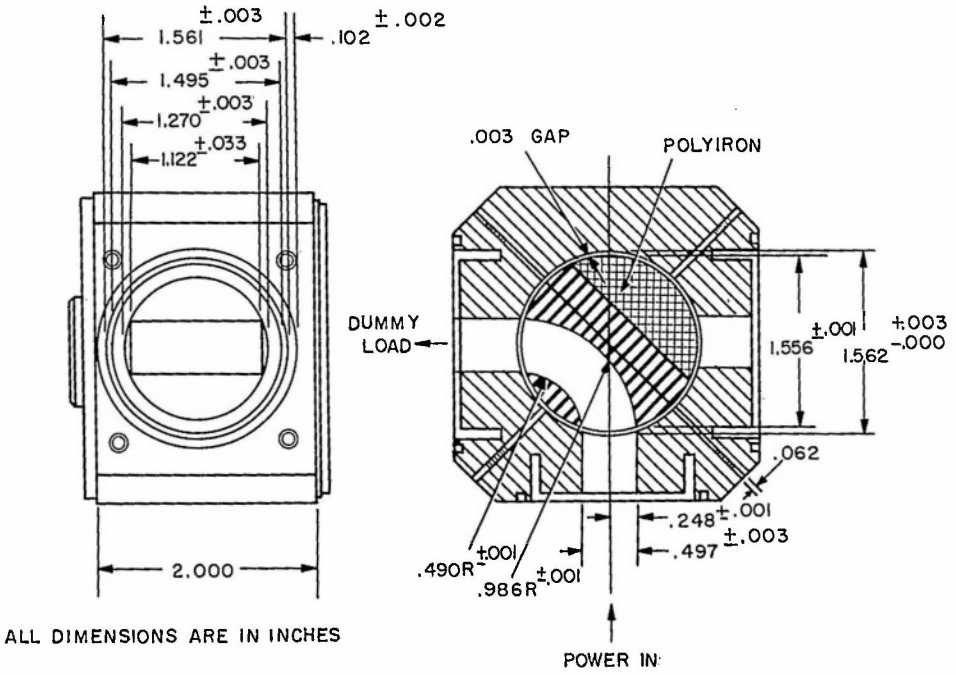

FIGURE 12

WAVEGUIDE SWITCH, DIMENSIONAL DRAWING

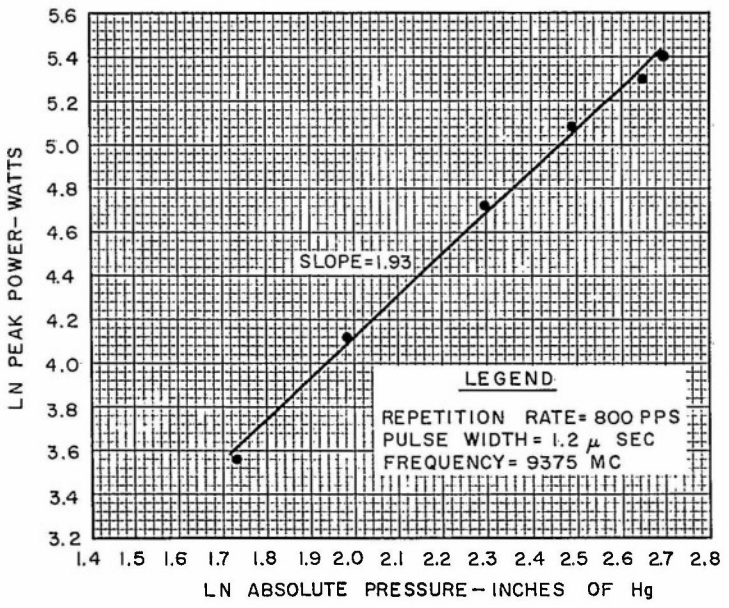

FIGURE 13

POWER VS PRESSURE FOR
WAVEGUIDE SWITCH AND DUMMY LOAD
(1-1/4"X 5/8 X 0.064"WAVEGUIDE)

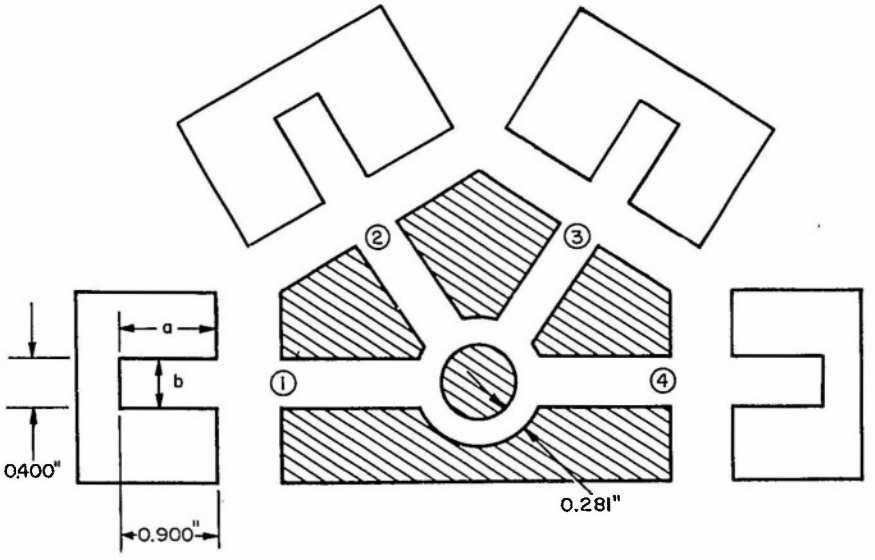

FIGURE 14

E-PLANE HYBRID RING

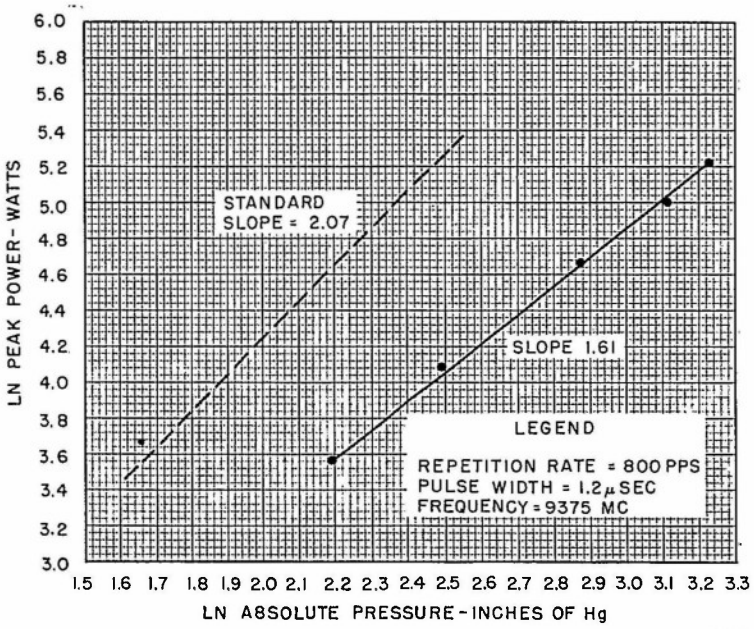

FIGURE 15

POWER VS PRESSURE
FOR HYBRID RING
(1"X 1/2"X 0.050" WAVEGUIDE)

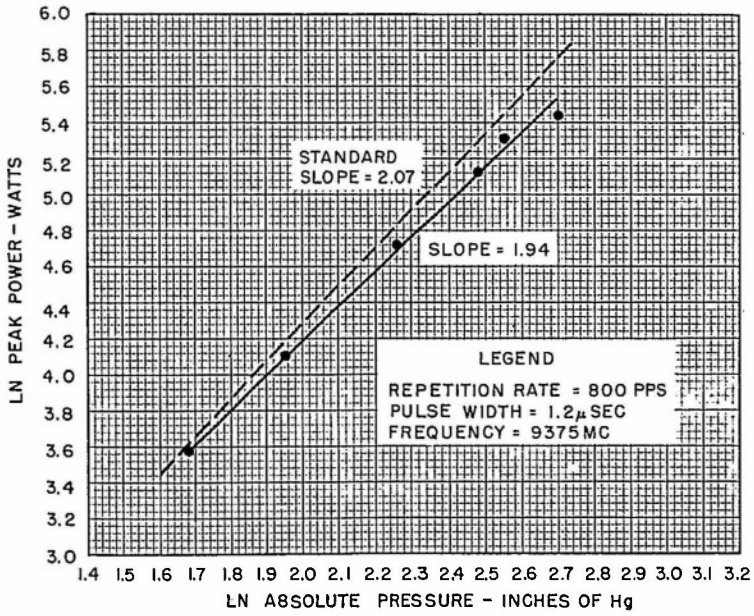

FIGURE 16

POWER VS PRESSURE
FOR 300-400 RMS FINISH
(1"X 1/2"X 0.050" WAVEGUIDE)

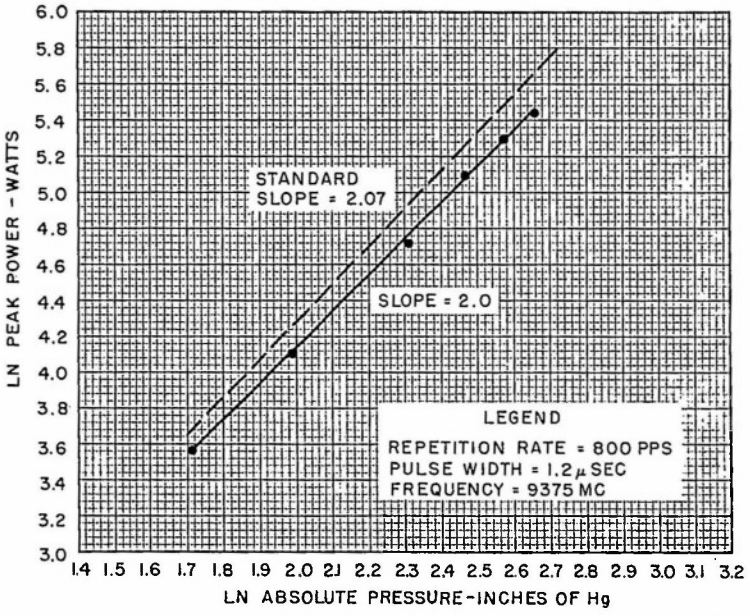

FIGURE 17

POWER VS PRESSURE
FOR 550-650 RMS FINISH
(1"X 1/2" X 0.050" WAVEGUIDE)

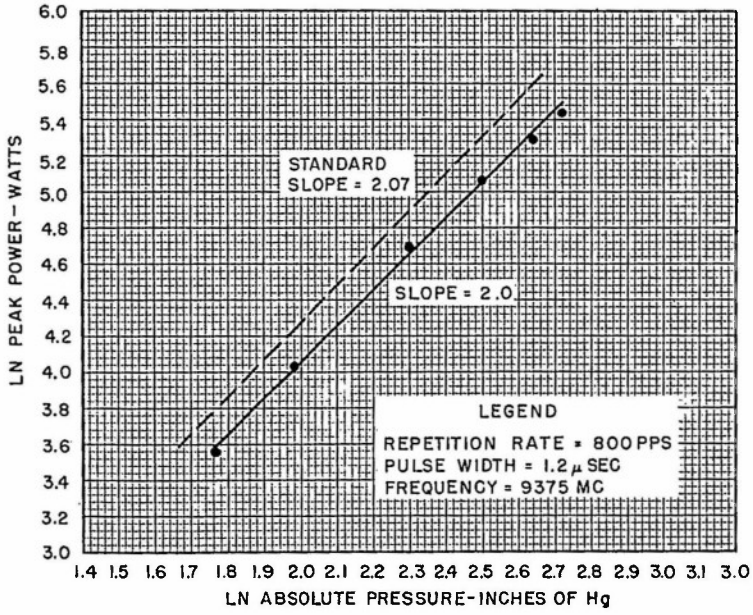

FIGURE 18

POWER VS PRESSURE
FOR 650-850 RMS FINISH
(1"X 1/2"X 0.050 WAVEGUIDE)

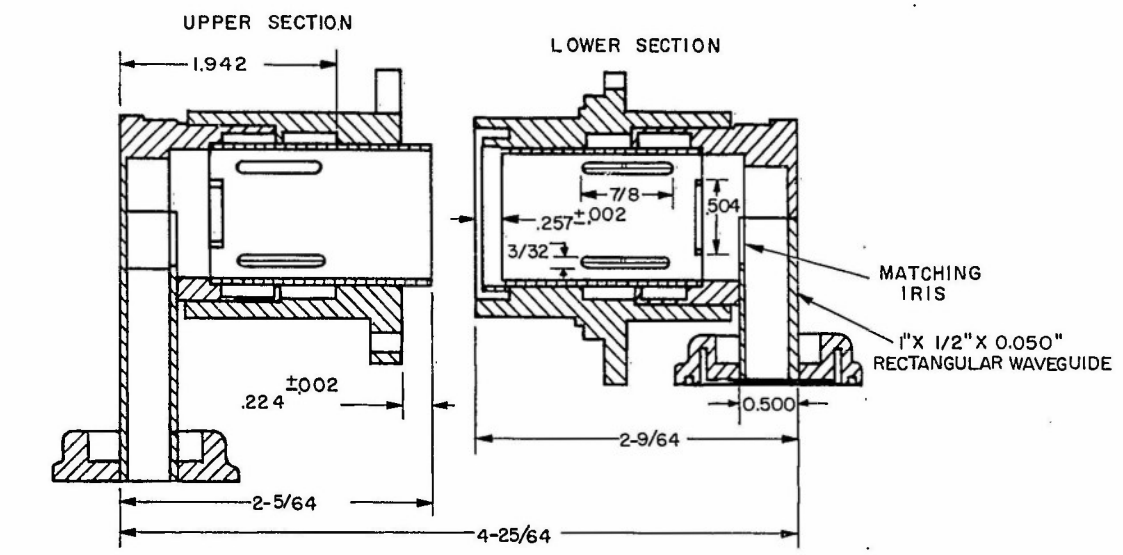

ALL DIMENSIONS ARE IN INCHES

FIGURE 19

RECTANGULAR-TO-CIRCULAR WAVEGUIDE ROTARY JOINT

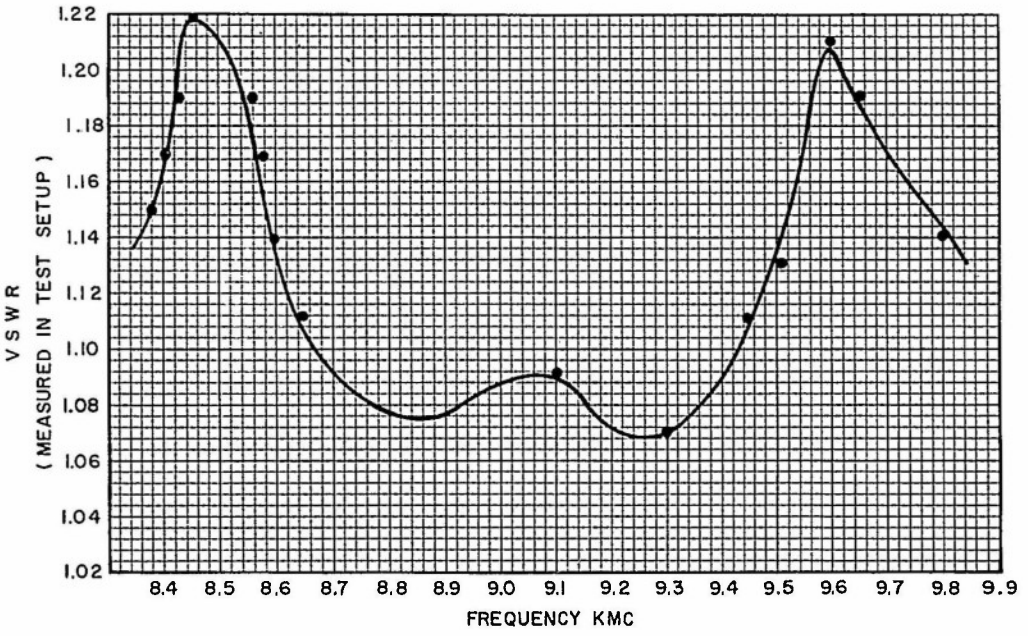

FIGURE 20

VSWR VS FREQUENCY FOR ROTARY JOINT (1"X1/2"X0.050" WAVEGUIDE)

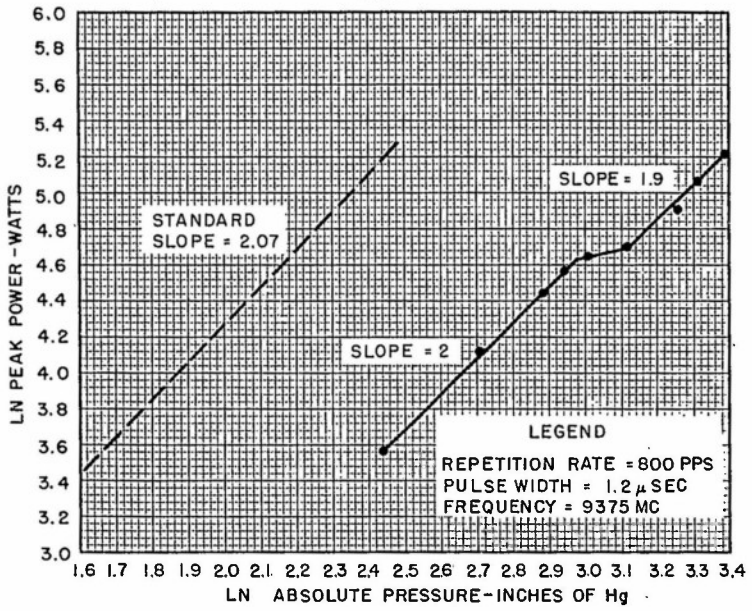

FIGURE 21
POWER VS PRESSURE FOR
ROTARY JOINT
(1"X 1/2"X 0.050" WAVEGUIDE)

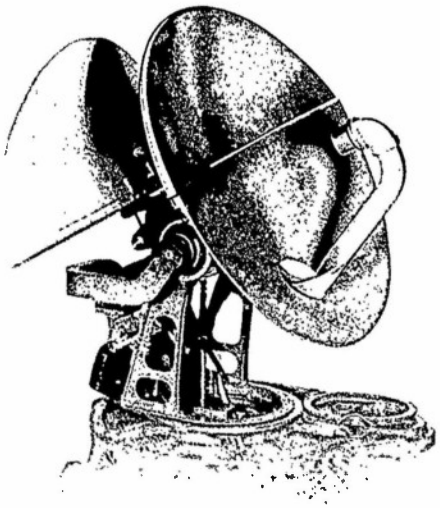

FIGURE 22
PHOTOGRAPH OF ANTENNA ASSEMBLY

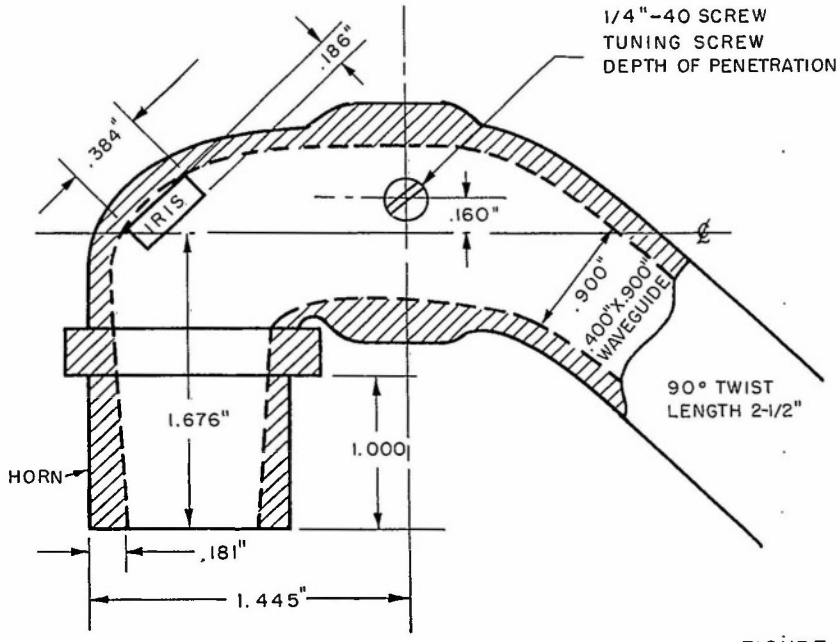

FIGURE 23

SKETCH OF ANTENNA ASSEMBLY
MICROWAVE COMPONENTS

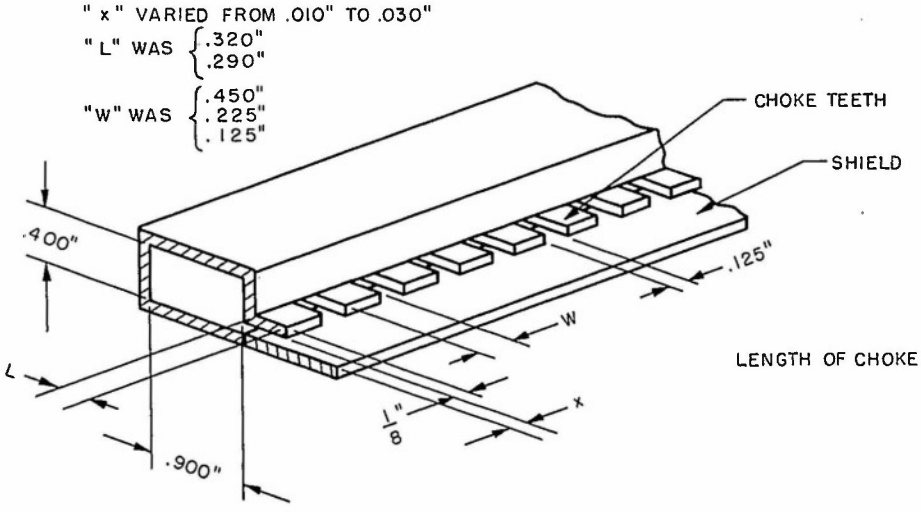

FIGURE 24

SKETCH OF LONGITUDINAL
SERRATED CHOKE

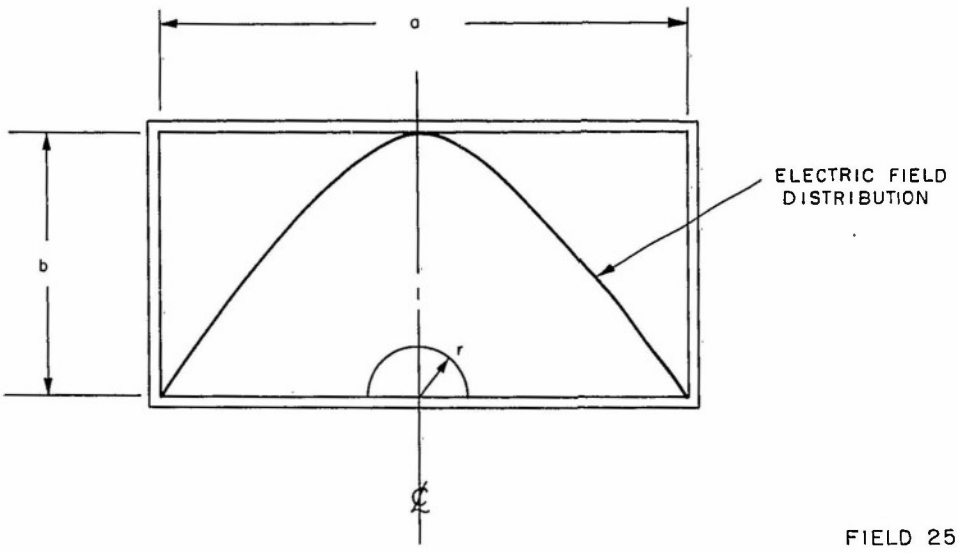

FIELD 25

CURVE OF ELECTRIC FIELD DISTRIBUTION

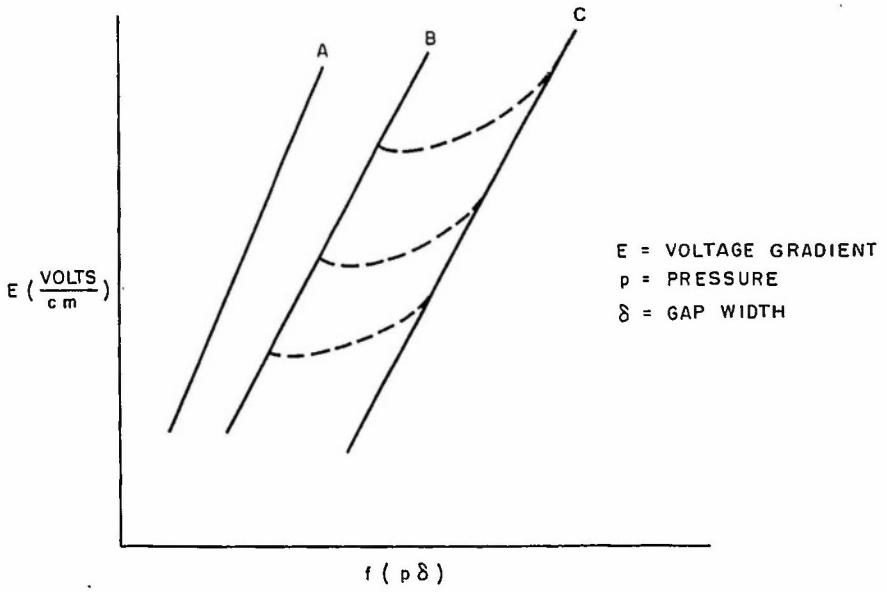

FIGURE 26

SKETCH OF PASCHEN'S LAW

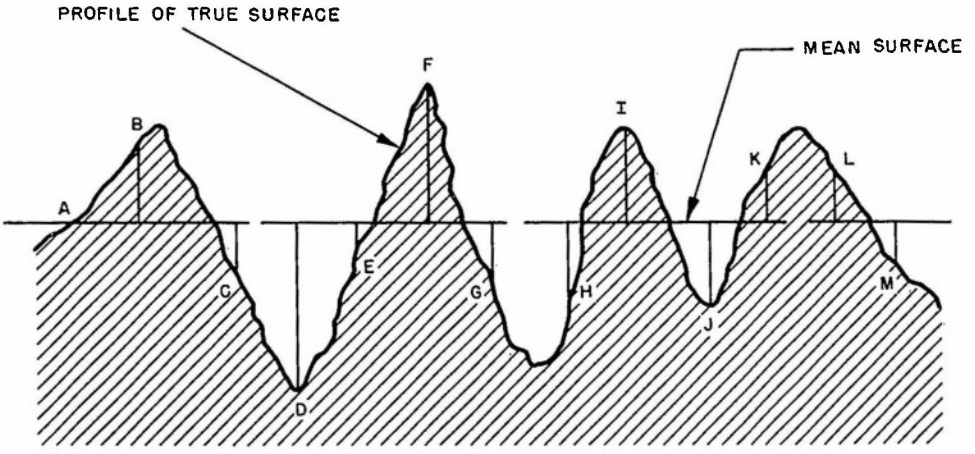

FIGURE 27
MEASUREMENT OF
SURFACE ROUGHNESS

SPERRY GYROSC
PROJECT PERFORMANCE AI
INDEX NO. NE-

CONTRACT NO. NObsr-52227

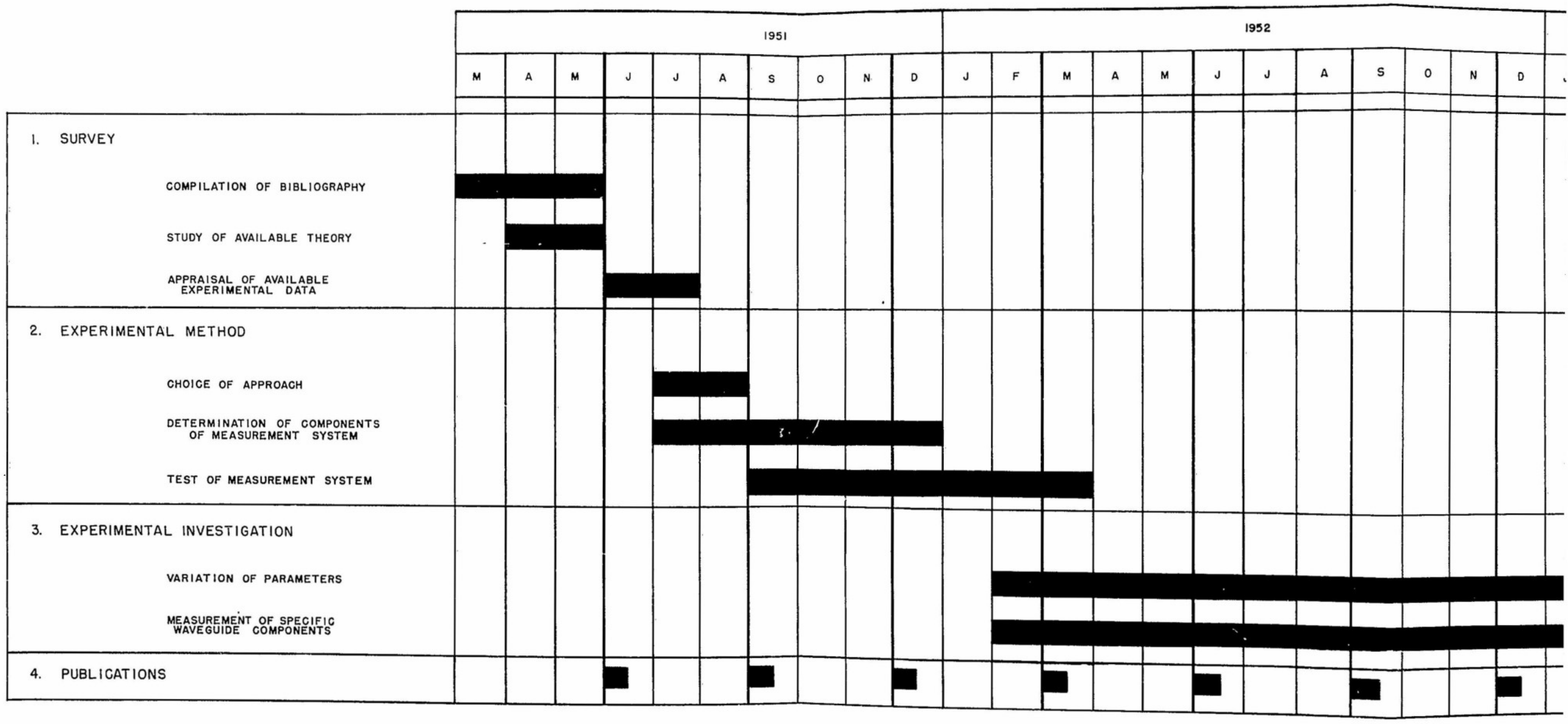

SPERRY GYROSCOPE COMPANY

PROJECT PERFORMANCE AND SCHEDULE CHART

INDEX NO. NE—110607

CONFIDENTIAL

PERIOD COVERED: 1 DECEMBER 1953 TO 28 FEBRUARY 1954

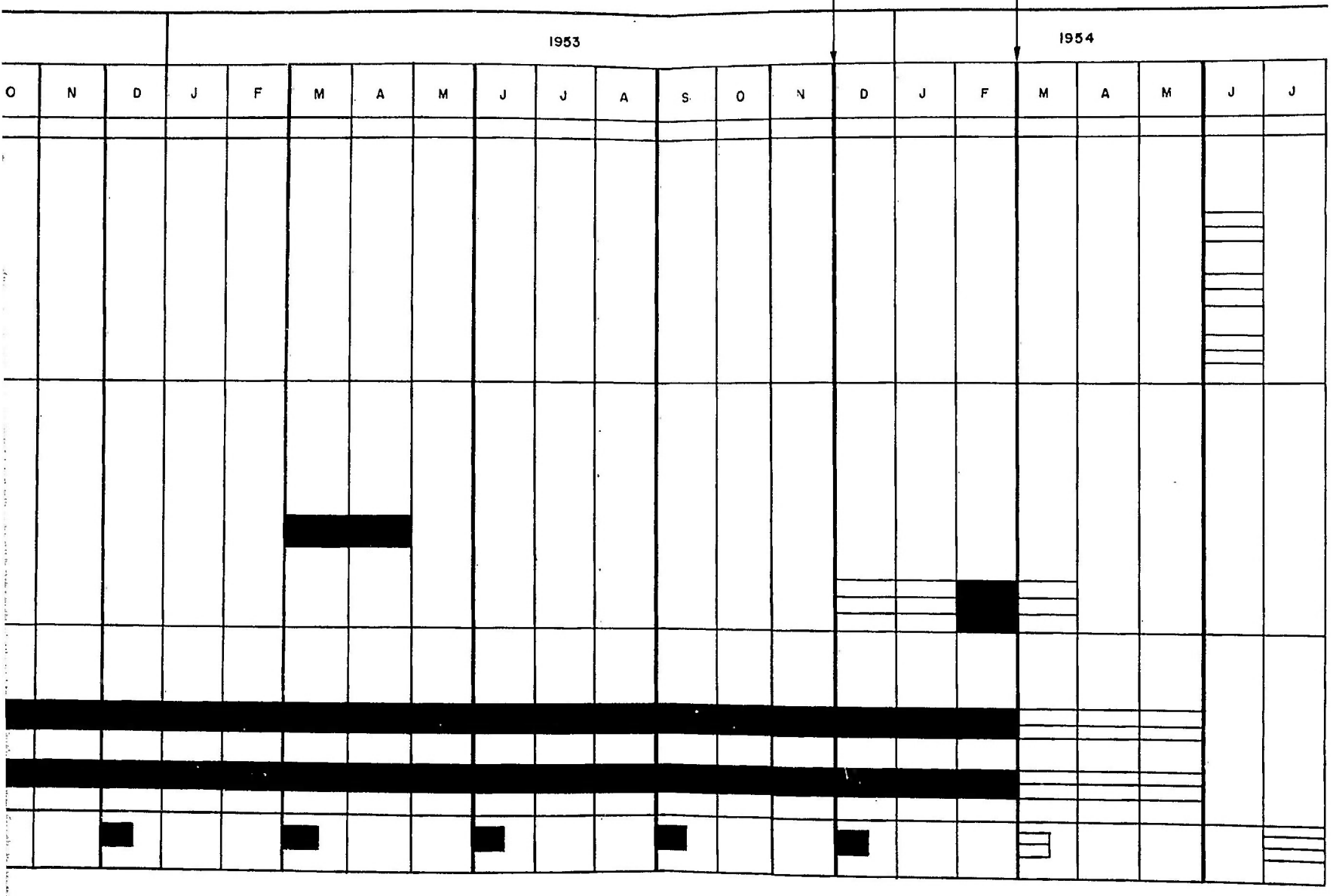

LEGEND: —

WORK PERFORMED

SCHEDULE OF PROJECTED OPERATION

ITEM: —

ESTIMATED COMPLETION IN PERCENT OF TOTAL EFFORT EXPECTED TO BE EXPENDED (NOT CHRONOLOGICAL)

1. SURVEY	90 %
2. EXPERIMENTAL METHOD	85 %
3. EXPERIMENTAL INVESTIGATION	70 %

NOTES AND REMARKS —

THIS SCHEDULE AND ESTIMATE APPLIES TO THE ANTICIPATED EXTENDED PROGRAM WHICH INCLUDES MEASUREMENTS IN TWO DIFFERENT SIZE WAVEGUIDES. THIS PROGRAM WILL END JUNE 15, 1954.

FIGURE 28

PROJECT PERFORMANCE AND SCHEDULE CHART

CONFIDENTIAL

CONFIDENTIAL